

Study on the Mechanical Properties of Carbon Dioxide Mineralization-Cured Alkali-Activated Rice Husk Ash Cementitious Composites

Ningxin Huang¹, Xinyong Wei¹, Yibo Mao¹, Yu Pang¹

(1. School of Civil Engineering and Architecture, Anhui University of Science and Technology, Huainan, Anhui 232001, China;)

Abstract: To investigate the mechanical properties of alkali-activated rice husk ash cementitious composites under Carbon Dioxide mineralization curing, this study systematically examined the effects of rice husk ash (RHA) content (0%, 5%, 7%, 10%), Carbon Dioxide mineralization curing duration (0, 60, 120, 200 min), and freeze-thaw cycles (0, 5, 15, 30) on compressive strength and durability through uniaxial compression tests and freeze-thaw resistance experiments. Microstructural evolution mechanisms were elucidated via X-ray diffraction (XRD) and scanning electron microscopy (SEM). Results demonstrate that specimens with 5% RHA content and 120 min Carbon Dioxide mineralization curing, activated by a sodium silicate solution (modulus = 2), achieved a 28-day compressive strength of 32.18 MPa, representing a 37.79% enhancement compared to the control group. After 30 freeze-thaw cycles, the strength loss rate remained below 23%. XRD and SEM analyses revealed that calcite (Calcium Carbonate) generated during Carbon Dioxide mineralization filled pore structures, inhibiting frost damage by reducing water penetration, while amorphous Silicon Oxide in RHA facilitated continuous pozzolanic reactions to form C-S-H gels, establishing a synergistic frost resistance mechanism. This research provides theoretical and technical insights for developing low-carbon building materials in cold regions. Non-linear relationships were observed between material performance and key parameters: compressive strength and freeze-thaw resistance initially increased and then decreased with prolonged mineralization duration, whereas increasing RHA content induced an initial decline followed by subsequent improvement in performance.

Keywords: Mineralization curing; Alkali activation; Rice husk ash; Cementitious composites; Freeze-thaw cycles; Mechanical properties; Microstructural mechanisms

1. INTRODUCTION

In recent years, the global construction industry has faced significant challenges in pursuing sustainable development. In 2021, China's construction sector accounted for 4.07 billion tons of carbon emissions, with cement production alone contributing 7% of global carbon emissions due to its high energy consumption and substantial Carbon Dioxide release, exacerbating greenhouse effects and environmental degradation. Driven by the "dual-carbon" objectives (carbon peaking and carbon neutrality), the development of low-carbon cementitious materials and carbon capture/utilization technologies has emerged as a pivotal strategy for the transformation of the building materials industry.

China produces over 40 million tons of rice husk annually. While direct incineration of rice husk generates underutilized ash with adverse environmental impacts, calcined rice husk ash (RHA)—after organic component removal—exhibits chemical and physicochemical properties comparable to reactive supplementary cementitious materials like silica fume, offering a cost-effective and abundant alternative to conventional cement. However, traditional curing methods fail to fully exploit its potential. Carbon Dioxide mineralization curing technology, which converts Carbon Dioxide into stable carbonate minerals via reactions between alkaline cementitious materials and Carbon Dioxide to form calcite (Calcium Carbonate), enables permanent Carbon Dioxide sequestration while enhancing the early-age strength and durability of cement-based composites.

In traditional Portland cement production, energy consumption and Carbon Dioxide emissions during limestone calcination and clinker sintering account for 60–70% of total emissions, posing a critical barrier to low-carbon transition. Alkali-activated cementitious materials, as a sustainable alternative, utilize industrial solid wastes rich in aluminosilicate components to form binding gels, reducing carbon emissions by 60–80%. RHA, an agricultural by-product rich in amorphous SiO₂, serves as an ideal silica source for alkali-activated systems. Nevertheless, alkali-activated RHA systems face technical challenges such as uncontrollable setting times and high shrinkage rates. Recent studies suggest that integrating Carbon Dioxide mineralization curing can regulate hydration kinetics: Carbon Dioxide reacts with Calcium ion to precipitate calcite, accelerating microstructural densification while compensating for shrinkage via volumetric expansion, thereby synergistically enabling efficient Carbon Dioxide mineralization. Existing research predominantly focuses on standalone mineralization or alkali activation, with limited exploration of their synergistic effects and freeze-thaw durability mechanisms.

This study investigates the mechanical performance of Carbon Dioxide mineralization-cured alkali-activated RHA cementitious composites. Through systematic experimentation and microstructural characterization, the research aims to reveal the influence mechanisms of RHA content, mineralization duration, and freeze-thaw cycles on material properties, providing theoretical foundations for developing high-performance, eco-friendly cementitious materials.

2. EXPERIMENTAL DESIGN

2.1 Raw Materials

Ordinary Portland cement (Grade 42.5) produced by Huainan Bagongshan Cement Plant was employed as the primary binder. Laboratory tap water served as the mixing water. Fine sand with a fineness modulus of 1.71 was used as the aggregate. Carbon Dioxide gas with 99.99% purity was supplied for mineralization curing. The alkaline activator was formulated by blending sodium silicate solution (Sodium Silicate, modulus=2) with sodium hydroxide (Sodium Hydroxide) pellets. Rice husk ash (RHA), primarily composed of amorphous Silicon Dioxide and Aluminum Oxide as confirmed by X-ray diffraction (XRD) analysis (Fig-1), was incorporated as a supplementary cementitious material.

Table-1 Physical properties of RHA

Category	Color	Specific surface area (m ² /kg)	Average diameter (μm)	SiO ₂ content (%)	Density (g/cm ³)
RHA	Grayish-white	62,100	4.25	≥84	2.4

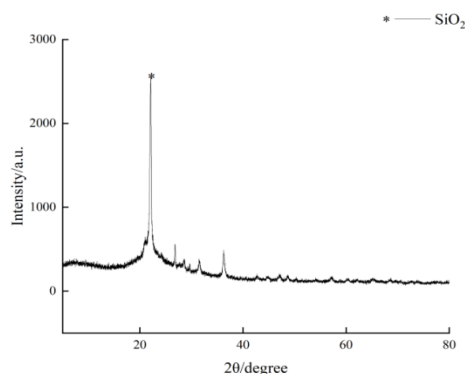


Fig-1. The XRD plot of rice husk ash

2.2 Mixing Ratio

The experimental mix proportions were designed based on orthogonal experimental methodology, with rice husk ash (RHA) content as the primary variable. Key parameters included a water-to-cement (W/C) ratio of 0.44 and a cement-to-sand (C/S) ratio of 0.68. RHA was incorporated as a partial cement replacement at 0%, 5%, 7%, and 10% by mass. Detailed mix formulations are provided in Table-2.

Table-2 Specific Mix Ratios (unit: kg/m³)

Group	Water	Sand	Cement	RHA	Alkali activator modulus
A0	80.21	258.96	178.51	0	2
A1	80.21	258.96	169.60	8.93	2
A2	80.21	258.96	166.02	12.49	2
A3	80.21	258.96	160.67	17.86	2

2.3 Specimen Preparation

Four groups of specimens with distinct mix proportions were prepared, including a control group without rice husk ash (RHA) and groups with RHA replacing cement at 0%, 5%, 7%, and 10% (denoted as A0, A1, A2, and A3, respectively). Raw materials, including RHA, cement, sand, and water, were meticulously proportioned. Cylindrical molds (50 mm × 100 mm) were uniformly coated with lubricant to facilitate demolding.

A two-stage dry-wet mixing procedure was employed:

1. Dry mixing: Cementitious materials and aggregates were blended in a mixer (300 rpm) for 50 s.
2. Wet mixing: An alkaline activator solution was introduced, followed by 60 s of mixing to ensure homogeneous paste formation.

The fresh mortar was then cast into molds and compacted on a vibration table (50 Hz frequency) until air bubbles were fully expelled. Specimen surfaces were leveled immediately after vibration.

For each mix proportion, four replicates were prepared. After casting, specimens were cured in a controlled chamber for 24 h, demolded, and subjected to Carbon Dioxide mineralization curing for 0, 60, 120, or 200 min. Subsequently, specimens were transferred to a standard curing chamber (constant temperature and humidity) for 28 days. Prior to freeze-thaw cycling tests, specimens were water-saturated for 4 days.

2.4 Test specimen design

Compressive Strength Testing: Compressive strength testing was conducted in accordance with GB/T 17671-2021 "Method for Testing Cement Mortar Strength". Specimens cured to designated ages were axially loaded on a compression testing machine with parallel surfaces aligned. Triplicate measurements were averaged as the test result. If any individual value deviated by more than ±10% from the mean, it was discarded, and the remaining values were re-averaged to determine the final compressive strength.

Freeze-Thaw Cycling Test: Freeze-thaw resistance was evaluated following GB/T 50082-2009 "Standard for Long-Term Performance and Durability Testing of Ordinary Concrete". The freeze-thaw regime comprised alternating cycles between $-20 \pm 2^\circ\text{C}$ (freezing) and $20 \pm 2^\circ\text{C}$ (thawing), with each phase lasting 4 hours, totaling 8 hours per cycle. Specimens with four distinct mix proportions underwent 0, 5, 15, and 30 freeze-thaw cycles.

X-Ray Diffraction Analysis: Phase composition evolution during freeze-thaw cycles was characterized using an X-ray diffractometer. Pre-dried specimens were pulverized into powders and analyzed with a scanning range of $5-70 (2\theta)$ at $2/\text{min}$.

Scanning Electron Microscopy (SEM): Fractured fragments from compressive tests were selected for microstructural analysis. Hydration reactions were terminated by immersion in anhydrous ethanol, followed by drying in a vacuum oven at 50°C for 24 h. Surface morphology and elemental distribution were examined using a field-emission SEM operated with samples sputter-coated with gold to enhance conductivity.

3. EXPERIMENTAL RESULTS AND DISCUSSION

3.1 Analysis of compressive strength of cement-based materials under different Carbon Dioxide mineralisation

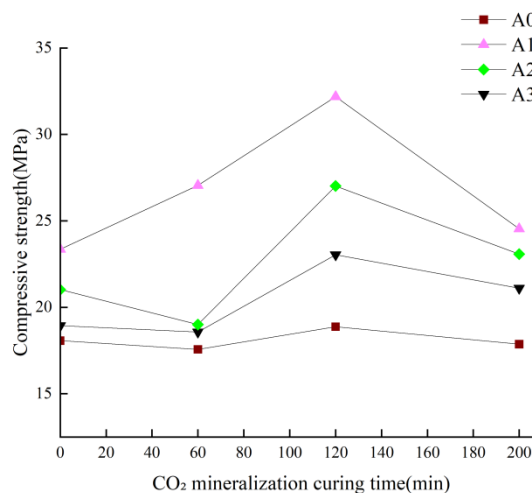


Fig-2 Compressive strength of cement-based materials under different Carbon Dioxide mineralization curing times

Fig-2 illustrates the influence of Carbon Dioxide mineralization curing duration on the compressive strength of alkali-activated rice husk ash (RHA) cementitious composites. As shown in Fig-2, the compressive strength initially increased and subsequently decreased with prolonged Carbon Dioxide mineralization curing. The maximum strength was achieved at 120 min of Carbon Dioxide curing, with all mineralized specimens exhibiting higher compressive strengths than the control group. At this optimal duration, the compressive strengths of specimens A0, A1, A2, and A3 reached 18.878 MPa, 32.183 MPa, 27.015 MPa, and 23.044 MPa, respectively, corresponding to increases of 4.47%, 37.79%, 28.50%, and 21.64% compared to the control group.

- These results demonstrate that early-stage Carbon Dioxide mineralization significantly enhances the mechanical performance of cementitious materials. This can be attributed to two synergistic mechanisms:

- Accelerated hydration kinetics: Carbon Dioxide reacts with Calcium ions in the alkaline matrix to precipitate nano-sized calcium carbonate (Calcium Carbonate), which refines pore structures and increases matrix density.
- Synergistic gel formation: The alkaline environment of RHA facilitates the dissolution of amorphous Silicon Dioxide and Aluminum Oxide, promoting the generation of calcium silicate hydrate (C-S-H) gels. Concurrently, Carbon Dioxide mineralization enhances the pozzolanic reactivity of RHA, leading to co-precipitation of Calcium Carbonate and C-S-H gels, thereby reinforcing the composite microstructure.

3.2 Analysis of compressive strength of cement-based materials with different rice husk ash content

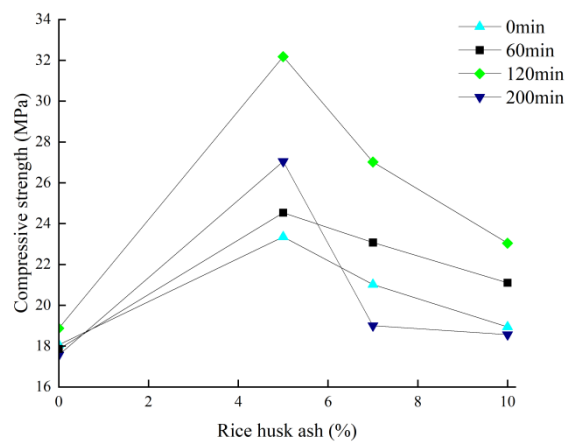


Fig-3 Compressive strength of cement-based materials with different rice husk ash content

Fig-3 demonstrates the effect of rice husk ash (RHA) content on the compressive strength of Carbon Dioxide mineralization-cured alkali-activated cementitious composites. As depicted in Fig-3, compressive strength initially increased and then decreased with rising RHA content, peaking at 5% RHA incorporation. All mineralized specimens exhibited superior compressive strength compared to the control group. At this optimal RHA dosage, specimens A0, A1, A2, and A3 attained compressive strengths of 23.356 MPa, 32.183 MPa, 27.045 MPa, and 24.539 MPa, respectively, representing increases of 29.26%, 35.05%, 41.34%, and 27.20% relative to the control.

These findings confirm that RHA significantly enhances the compressive strength of cementitious materials through two synergistic mechanisms:

- Micro-aggregate effect: RHA particles (<50 μm) fill interfacial transition zone (ITZ) voids, reducing porosity and improving matrix compactness.
- Pozzolanic reactivity: Amorphous Silicon Dioxide and Aluminum Oxide in RHA react with calcium hydroxide (Calcium Hydroxide) under alkaline activation to form additional calcium silicate hydrate (C-S-H) and calcium aluminate silicate hydrate (C-A-S-H) gels, thereby accelerating hydration kinetics and strengthening the binder phase.

The combined effects of pore structure refinement and gel-phase augmentation account for the observed mechanical enhancement, with excessive RHA content (>5%) likely introducing unreacted particles that disrupt microstructural homogeneity.

3.3 Static uniaxial compression test of rice husk ash cement-based materials activated by alkaline mineralisation of carbon dioxide under freeze-thaw cycles

3.3.1 Analysis of compressive strength of rice husk ash cement-based materials activated by alkaline mineralisation of Carbon Dioxide under freeze-thaw cycles

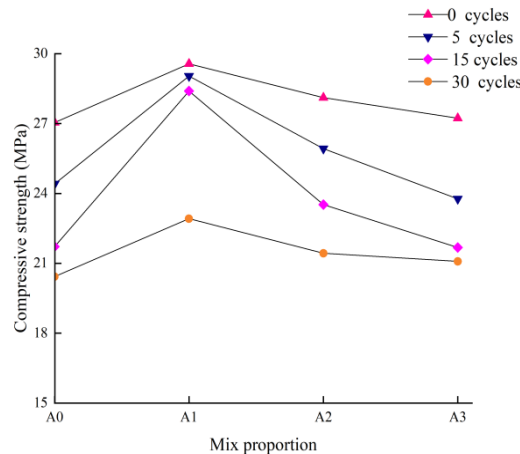


Fig-4 Compressive strength of cement-based materials under freeze-thaw cycles

Fig-4 presents the variation in 28-day compressive strength of alkali-activated rice husk ash (RHA) cementitious composites under freeze-thaw cycles, with specimens subjected to 120-minute Carbon Dioxide mineralization curing at varying RHA replacement levels (0%, 5%, 7%, and 10%). As shown in Fig-4, specimens with 5% RHA exhibited superior compressive strength compared to both the RHA-free control group and those with higher RHA dosages. Specifically, compressive strength increased with RHA incorporation up to 5% but declined at 7% RHA, though remaining higher than the control group. This nonlinear behavior is attributed to the dual roles of amorphous and crystalline Silicon Dioxide phases in RHA, governed by their particle size distribution and reactivity.

Freeze-Thaw Degradation Mechanism:

Compressive strength decreased progressively with freeze-thaw cycles, driven by:

- Frost heave stress: Water volume expansion (~9% upon freezing) generated internal tensile stresses, initiating microcracks.
- Capillary-ice cyclic damage: Thawing enabled water infiltration into newly formed cracks, followed by re-freezing-induced crack propagation, forming interconnected damage networks (Fig-1).

Post-30 cycles, compressive strengths of A0–A3 decreased to 20.427 MPa, 22.915 MPa, 21.432 MPa, and 21.081 MPa, corresponding to reductions of 24.47%, 22.50%, 25.15%, and 22.58%, respectively. The 5% RHA group demonstrated optimal frost resistance, attributed to its refined pore structure and minimal microcrack density, effectively mitigating cyclic damage.

- Microstructural Analysis:

Amorphous Silicon Dioxide: Improved durability via enhanced C-S-H gel formation and pore refinement.

- Crystalline Silicon Dioxide: Introduced interfacial defects, accelerating freeze-thaw deterioration at higher dosages.

This study highlights the critical balance between RHA reactivity and particle size in optimizing frost-resistant, Carbon Dioxide -mineralized cementitious materials.

3.3.2 Analysis of stress-strain curves of rice husk ash cementitious materials activated by Carbon Dioxide mineralisation curing alkali under freeze-thaw cycles

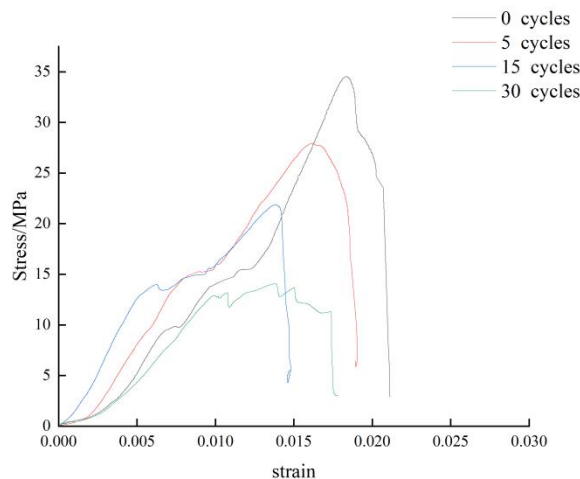


Fig-5 Stress-strain curve of cement-based materials under the freeze-thaw cycle

Fig-5 depicts the stress-strain curves of Carbon Dioxide mineralization-cured alkali-activated rice husk ash cementitious composites under varying freeze-thaw cycles (0, 5, 15, and 30 cycles). All curves exhibit a unimodal pattern, characteristic of quasi-brittle materials, indicating significant plastic deformation prior to failure. Analogous to conventional cement-based materials, the deformation process comprises four distinct phases: compaction, elastic deformation, crack propagation, and failure.

1. Compaction Phase:

- Stress increases nonlinearly with strain as inherent pores are gradually compressed, enhancing matrix densification.
- Calcite (Calcium Carbonate) generated during Carbon Dioxide mineralization partially counteracts freeze-thaw-induced pore expansion. However, prolonged freeze-thaw cycling shortens this phase, reflecting reduced initial compactness due to cumulative frost damage.

2. Elastic Deformation Phase:

- A near-linear stress-strain relationship emerges, with a discernible elastic modulus.
- Progressive freeze-thaw cycles degrade interfacial bonding between calcium silicate hydrate (C-S-H) gels and aggregates, leading to a decline in elastic modulus.

3. Crack Propagation Phase:

- Curve slope increases as internal microcracks initiate and propagate. Calcite deposits delay crack coalescence but cannot fully offset cyclic frost heave stresses.

- Repeated freeze-thaw cycles induce cumulative microcrack networks (increased length and density), diminishing load-bearing capacity.

4. Failure Phase:

- Post-peak stress, the curve enters a descending branch, marked by rapid stress reduction and macroscopic failure.
- Brittleness intensifies with freeze-thaw cycles due to enhanced crack connectivity and localized breakdown of calcite pore-filling effects.

Peak Stress Degradation Mechanism:

Peak stress declines with increasing freeze-thaw cycles. While calcite initially mitigates porosity via pore filling, its efficacy diminishes under prolonged cyclic loading. Key mechanisms include:

- Frost heave stress: Water volume expansion (~9%) during freezing generates multidirectional tensile stresses, driving crack nucleation.
- Capillary-ice cyclic damage: Thawing enables water infiltration into new cracks, followed by re-freezing-induced expansion, accelerating interfacial debonding between gels and aggregates.
- Pore-coalescence: Progressive crack extension and porosity amplification weaken structural integrity, ultimately reducing compressive strength.

This study elucidates the interplay between Carbon Dioxide mineralization benefits and frost-induced deterioration, emphasizing the critical role of microstructural stability in cold-region cementitious material design.

3.3.3 Analysis of the energy characteristics of rice husk ash cement-based materials activated by Carbon Dioxide-mineralisation under freeze-thaw cycles

The energy characteristics were analyzed based on the First and Second Laws of Thermodynamics, with fundamental equations given as Eqs. (1)–(3):

$$U = \int_0^{\varepsilon_i} \sigma_i \, d\varepsilon_i \quad (1)$$

$$U_e = \frac{\sigma_i^2}{2E_e} \quad (2)$$

$$U_d = U - U_e \quad (3)$$

Where:

U=total energy

U_e =elastic energy

U_d =dissipative energy

ε_i =axial strain

σ_i =axial stress

E_e =elastic modulus.

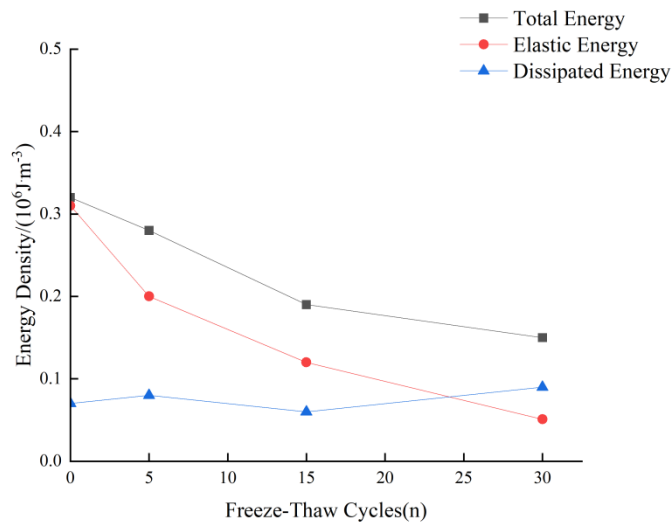


Fig-6 Energy characteristic curves of cement-based materials under freeze-thaw cycles

Fig-6 illustrates the energy characteristic curves of cementitious composites with 120-minute Carbon Dioxide mineralization curing and 5% rice husk ash (RHA) content under progressive freeze-thaw cycles. Key observations include:

Energy Evolution Trends

1. Total Energy and Elastic Energy Decline:

- Total energy and elastic energy decreased monotonically with increasing freeze-thaw cycles.
- Non-cycled specimens exhibited the highest total energy, attributed to their initial dense microstructure and synergistic pore-filling effects from calcite (Calcium Carbonate) generated during Carbon Dioxide mineralization.

2. Dominance of Elastic Energy (0 cycles):

- Elastic energy accounted for >80% of total energy, indicating predominant elastic deformation during early loading.
- Strong interfacial bonding between calcium silicate hydrate (C-S-H) gels and aggregates, coupled with limited microcrack propagation, facilitated efficient elastic strain energy storage.
- Low dissipation energy (<20%) reflected minimal plastic deformation and crack growth, confirming high material integrity.

Stage-Specific Degradation Mechanisms

1. After 5 Freeze-Thaw Cycles:

- Total energy decreased by 18.5%, with elastic energy contribution dropping to ~70% and dissipation energy rising to ~30%.
- Initial frost heave stresses induced localized microcracks, though calcite pore filling and ongoing pozzolanic reactions of amorphous SiO₂ in RHA partially repaired interfacial debonding via C-S-H gel regeneration.

2. After 15 Freeze-Thaw Cycles:

- Total energy declined sharply (42.3% reduction vs. 0 cycles), with dissipation energy exceeding 35%.
- Cyclic "infiltration-freezing-expansion" effects generated multidirectional tensile stresses, accelerating crack propagation.
- Localized fracture of calcite fillers and weakened gel-aggregate bonding reduced synergistic mitigation efficacy, despite partial damage compensation by RHA-derived C-S-H gels.

3. After 30 Freeze-Thaw Cycles:

- Total energy reached its minimum (55.8% reduction vs. 0 cycles), with dissipation energy dominating (>45%) and elastic energy contribution falling below 40%.
- Highly interconnected cracks and exacerbated brittleness indicated advanced damage, characterized by macro-crack networks and irreversible loss of structural cohesion.

This analysis quantifies the competing mechanisms between Carbon Dioxide mineralization benefits and frost-induced deterioration, providing critical insights for optimizing freeze-thaw-resistant cementitious materials.

3.3.4 Analysis of the failure modes of rice husk ash cement-based materials activated by Carbon Dioxide-mineralisation curing under freeze-thaw cycles

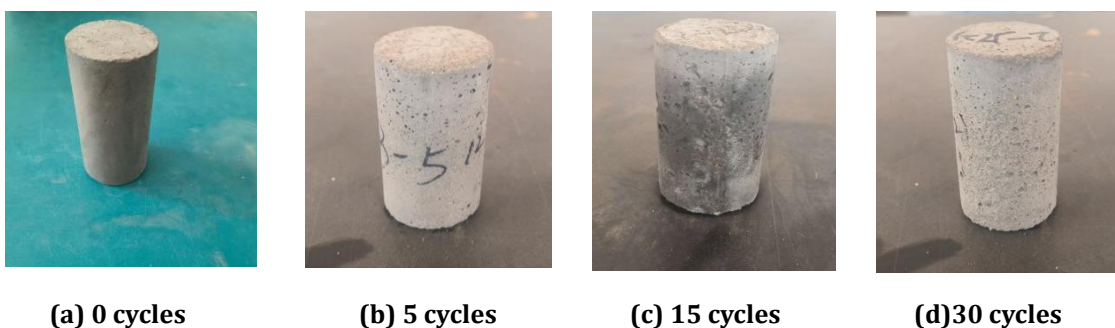


Fig-7 Microstructural diagram of cement-based materials under freeze-thaw cycles

Fig-7 illustrates the progressive surface damage evolution of alkali-activated rice husk ash (RHA) cementitious composites subjected to Carbon Dioxide mineralization curing (120 min) with 5% RHA replacement under increasing freeze-thaw cycles (0, 5, 15, and 30 cycles). The macroscopic morphological changes, as depicted in Fig-9(a)–Fig-9(d), reveal distinct stage-dependent degradation patterns:

0 cycles (Fig-9a):

- Specimens exhibited intact surfaces with smooth texture and sharp edges, indicating negligible initial defects.
- Structural integrity was preserved by the dense matrix reinforced by calcite (Calcium Carbonate) precipitation from Carbon Dioxide mineralization.

5 cycles (Fig-9b):

- Scattered micro-pits and slight edge rounding emerged, though the overall geometry remained intact.
- Localized frost heave stresses initiated minor surface erosion, partially mitigated by calcite pore-filling effects.

15 cycles (Fig-9c):

- Pitting density and size increased significantly, accompanied by pronounced edge rounding and localized aggregate exposure.
- Cyclic "infiltration-freezing-expansion" mechanisms exacerbated interfacial debonding, compromising surface cohesion.

30 cycles (Fig-9d):

- Severe macro-damage manifested as extensive spalling, rounded edges, deep erosion zones, and prominent aggregate protrusion.
- Interconnected microcracks propagated into macrocracks, reflecting irreversible structural disintegration.
- Mechanistic Interpretation:
The observed damage progression—from localized micro-defects to global structural failure—correlates with cumulative frost-induced stresses overwhelming the composite's self-healing capacity. Key factors include:
 - Calcite degradation: Progressive disruption of Calcium Carbonate pore-blocking networks under cyclic loading.
 - RHA limitations: Despite amorphous Silicon Dioxide's pozzolanic reactivity, C-S-H gel regeneration rates were insufficient to counteract accelerated crack propagation at advanced freeze-thaw stages.

This morphological analysis underscores the critical threshold (15–30 cycles) beyond which Carbon Dioxide mineralization and RHA synergies fail to sustain material durability, providing actionable insights for frost-resistant material design.

3.3.5 XRD Experiment and Analysis of Cement-Based Materials Under Freeze-Thaw Cycles

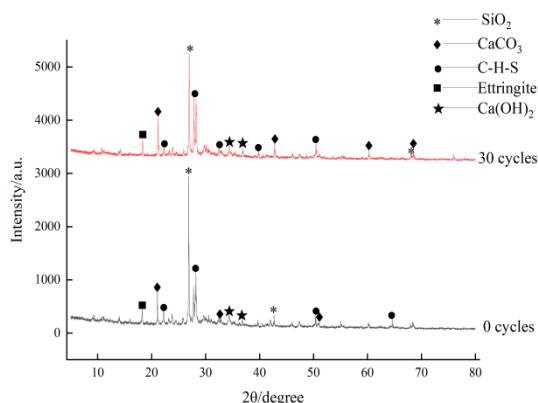
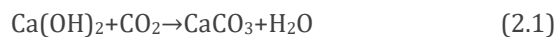
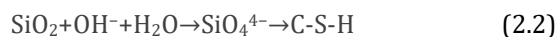


Fig-8 XRD pattern of cement-based materials under freeze-thaw cycles

Fig-8 shows the XRD patterns of Carbon Dioxide mineralisation-cured alkaline-activated rice husk ash cement-based materials after 0 freeze-thaw cycles and 30 freeze-thaw cycles. As can be seen from the figure, the XRD patterns of the unfrozen specimens show significant calcite diffraction peaks around 29.4° , indicating that Carbon Dioxide mineralisation curing effectively solidified Carbon Dioxide. In comparison, after 30 freeze-thaw cycles, the intensity of the Calcium Hydroxide diffraction peaks in the specimens was slightly higher than that in the unfrozen specimens, attributed to the formation of cracks inside the specimens due to freeze-thaw cycles, exposed unreacted Calcium Hydroxide and free Calcium Ions react with Carbon Dioxide in the later stages to undergo secondary mineralisation (Equation 2.1), re-forming Calcium Carbonate and partially offsetting mineral dissolution.



The intensity of the Silicon Oxide diffraction peak decreased after freeze-thaw exposure, indicating a reduction in amorphous Silicon Oxide content or detectable crystalline phases. This may result from increased porosity due to freeze-thaw cycles, causing partial detachment of incompletely reacted RHA particles from cracks. Freeze-thaw actions also exacerbate interfacial debonding of unreacted particles in alkali-activated materials, making larger Silicon Oxide particles in RHA-concrete more susceptible to frost heave stress-induced detachment. Although partial gel structures are damaged during freeze-thaw cycles, moisture infiltration during thawing may reactivate the reactivity of residual amorphous Silicon Oxide in RHA, facilitating continuous pozzolanic reactions in the alkaline environment to form C-S-H gel (Eq. 2.2). Provis et al. noted that moisture migration during freeze-thaw cycles promotes dissolution and reprecipitation of silico-aluminate phases in alkali-activated systems, reducing amorphous Silicon Oxide content. Consequently, the XRD pattern after 30 cycles exhibits an intensified broadening peak ($2\theta = 27^\circ - 30^\circ$) for C-S-H gel.



The broadened C-S-H gel diffraction peak ($30^\circ - 35^\circ$) in unfrozen specimens reflects its amorphous structural characteristics. After 30 cycles, the peak width slightly increased, indicating loosened interlayer gel structures due to frost heave stress. These results demonstrate that calcite generated via Carbon Dioxide mineralization inhibits freeze-thaw water ingress by pore filling, while RHA supplies reactive silicon sources to promote gel regeneration, forming a dual mechanism of "calcite filling-gel self-healing."

- The pore structure optimization by calcite (Calcium Carbonate) via Carbon Dioxide mineralization can be further explained by the nucleation and growth theory. According to Wu et al., during the initial Carbon Dioxide mineralization stage, Calcium Ions and Carbonate form nuclei on pore surfaces under alkaline conditions, eventually developing dense calcite layers. This process is governed by mineralization time and Carbon Dioxide diffusion rates:
- Short mineralization time (<60 min): Low nucleation density and small crystal size limit pore-filling efficiency.
- Optimal mineralization time (120 min): Nuclei grow sufficiently to cover pore walls, significantly reducing pore connectivity.
- Excessive mineralization time (>120 min): Over-accumulation of calcite may cause localized stress concentrations and microcracks, leading to strength degradation (see Fig-2).

Furthermore, amorphous Silicon Oxide in RHA enhances nucleation by providing hydroxyl groups on its surface as active sites for Calcium Ions adsorption, accelerating nucleus formatio. Thus, the synergy between nucleation-growth

mechanisms and pozzolanic reactions is critical for improving compressive strength and frost resistance in cement-based materials.

3.3.6 Microscopic image of cement-based material under the action of freeze-thaw cycle

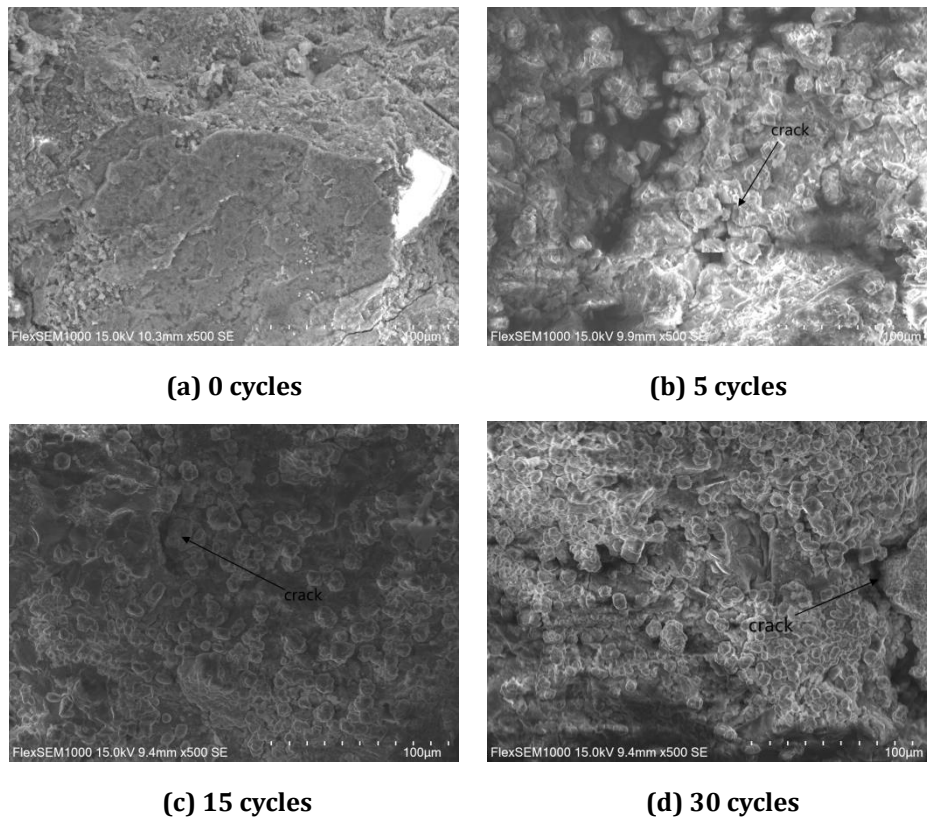


Fig-9 Microstructural diagram of cement-based materials under freeze-thaw cycles

Fig-9 reveals the progressive deterioration mechanisms of Carbon Dioxide mineralization-cured alkali-activated rice husk ash (RHA) cementitious composites under increasing freeze-thaw cycles. Key observations include:

As shown in Figure 9, the damage caused by frost heave forces to the interparticle cementation gradually intensifies with the increase in freeze-thaw cycles, leading to crack initiation and propagation within the specimen and ultimately resulting in structural failure. In the early stages of freeze-thaw cycles (e.g., 0–5 cycles), specimens cured with 120-minute Carbon Dioxide mineralization and containing 5% rice husk ash (RHA) exhibited dense internal structures due to the pore-filling effect of calcite (Calcium Carbonate) generated by Carbon Dioxide mineralization and the reinforcement of the matrix by C-S-H gel formed through the reaction of amorphous Silicon Dioxide in RHA [14]. This optimized microstructure, characterized by strong particle bonding and low porosity, showed no significant crystalline phases and maintained high structural integrity, thereby minimizing frost-induced damage.

As freeze-thaw cycles increased (e.g., 15–30 cycles), particle aggregation became evident within the specimens. This phenomenon arises from the repeated phase transition of pore water between liquid and solid states. During freezing, the volume expansion of water (approximately 9%) generates frost heave stresses, enlarging pores and exposing unreacted Calcium Hydroxide, which subsequently reacts with infiltrated Carbon Dioxide to form secondary calcite through carbonation. Concurrently, during thawing, water permeates into newly formed pores, eroding cementitious phases and

weakening interparticle bonds. This process leads to the detachment of larger crystalline Silicon Dioxide particles from RHA, forming isolated grains. Macroscopically, the porosity of the specimens increased significantly with freeze-thaw cycles, accompanied by progressive surface spalling. Specimens subjected to fewer freeze-thaw cycles retained partial interparticle contact, resulting in higher longitudinal wave velocities and compressive strengths, with relatively intact fracture surfaces and fewer debris particles post-failure.

Microscopically, the freeze-thaw deterioration of Carbon Dioxide -mineralized alkali-activated RHA cement-based materials is attributed to the synergistic effects of physical expansion (from water-ice phase transitions) and chemical erosion (e.g., gel dissolution). However, the synergistic interaction between calcite (from Carbon Dioxide mineralization) and RHA partially mitigates damage by delaying crack propagation. From a macroscopic perspective, frost heave forces predominantly manifest as triaxial tensile stresses, driven by the volumetric expansion of pore water during phase transitions, which generates multidirectional tensile stress fields within the material [15].

4.CONCLUSIONS

Using rice husk ash as a base material, water glass with a modulus of 2 was added to activate its reactivity. Carbon Dioxide mineralisation curing was employed to prepare Carbon Dioxide -mineralised cured alkali-activated rice husk ash cementitious materials. The compressive strength of the materials increased initially and then decreased with increasing rice husk ash content and mineralisation curing time. Excessive rice husk ash content adversely affects the strength of the cementitious materials, with an optimal rice husk ash content of 5%. Carbon Dioxide mineralisation curing time of 120 minutes resulted in cement-based materials with a compressive strength of 32.183 MPa at 28 days, representing a 37.8% increase compared to the control group. After 30 freeze-thaw cycles, the strength loss rate was below 23%, meeting the requirements for engineering applications in severely cold regions.

Carbon Dioxide mineralisation curing time significantly affects the compressive strength of cement-based materials, with 120 minutes being the optimal curing time, at which the maximum amount of calcite is formed, and the 28-day compressive strength reaches 32.18 MPa.

When the rice husk ash content is 5%, the material exhibits optimal comprehensive performance, with the microaggregate effect and volcanic ash activity synergistically enhancing density. Excessive addition (>7%) leads to strength reduction due to the aggregation of crystalline Silicon Oxide.

The peak strength, total energy, and elastic properties of cement-based materials decrease with increasing freeze-thaw cycle counts. Compared to unfrozen specimens, after 30 freeze-thaw cycles, the peak strength decreased by 22.50%, total energy decreased by 53.13%, and elastic properties decreased by 83.55%.

XRD and SEM analyses indicate that the synergistic effect of Carbon Dioxide mineralisation and rice husk ash increases Calcium Carbonate content and C-S-H gel regeneration rate after freeze-thaw cycles. The pore-filling effect of calcite crystals significantly reduces freeze-thaw water permeability, while the continuous volcanic ash reaction of amorphous Silicon Oxide in rice husk ash generates C-S-H gel, forming a 'physical barrier-chemical repair' synergistic freeze-resistance mechanism.

REFERENCES

1. Kai J ,Peta A . The development of Carbon Capture Utilization and Storage (CCUS) research in China: A bibliometric perspective [J]. Renewable and Sustainable Energy Reviews, 2020, (prepublish): 110521-.
2. Research Report on China Building Energy Consumption and Carbon Emission (2023) [J]. Construction, 2024, (02): 46-59.
3. China Blue Book on Climate Change (2022) was released [J]. China Environmental Monitoring, 2022, (08): 4.
4. Zhang Zhaohui, Lou Zongke. Current research status of rice husk and rice husk ash cement concrete [J]. Shanxi Agricultural Science, 2010,56 (06): 124-126.
5. Wu Shengkun, Huang Tianyong, Xie Yan, et al. Research progress of carbon dioxide mineralization and curing cement-based materials [J]. Silicate Bulletin, 2023,42 (06): 1897-1911. DOI:10.16552/j.cnki.issn1001-1625.20230508.001.
6. Provis L J ,Bernal A S . Geopolymers and Related Alkali-Activated Materials [J]. Annual Review of Materials Research, 2014, 44 (1): 299-327.
7. Ataie F F. Utilization of treated agricultural residue ash as sodium silicate in alkali activated slag systems[J]. Materials, 2021, 14(2): 329.
8. Huang Hao. Study on the mechanism of CO₂ mineralization and curing building materials based on hydrated inert cementing materials [D]. Zhejiang University, 2019. DOI:10.27461/d.cnki.gzjdx. 2019.001885.
9. Chen Shan, Wu Anran. Interpretation of new standard (GB / T 17671) [J]. Cement Engineering, 2021, (05): 22-24. DOI:10.13697/j.cnki.32-1449/tu.2021.05. 007.
10. Cold light glow, Rong Junming, Ding Wei, et al. Introduction to test methods standard for long-term performance and durability of ordinary Concrete GB / T50082-2009 [J]. Construction technology, 2010,39 (02): 6-9.
11. Chopra D, Siddique R, Kunal.Strength, permeability and microstructure of self-compacting concrete containing rice husk ash[J].Biosystems Engineering, 2015, 130: 72-80.
12. Liu Xianghua, Zhang Ke, Liu Wenlian. The effect of load and freeze-thaw on the energy conversion and damage characteristics of multi-fissure sandstone [J]. Journal of Applied Basic and Engineering Science, 2023,31 (03): 715-730. DOI:10.16058/j.issn.1005-0930.2023.03.015.
13. Provis L J ,Bernal A S . Geopolymers and Related Alkali-Activated Materials [J]. Annual Review of Materials Research, 2014, 44 (1): 299-327.
14. Zhou Yuwan, Chen Sili, Yang Kaifeng, et al. Effect of rice husk ash on the mechanical properties of cement-based materials [J]. Concrete, 2023, (08): 82-86.
15. Jia Hailiang, Liu Qingping, Xiang Wei, et al. Expansion model of saturated sandstone damage under freeze-thaw cycle [J]. Journal of Rock mechanics and Engineering, 2013,32 (S2): 3049-3055.